Fuel 210 (2017) 790–802

Contents lists available at ScienceDirect

Fuel

journal homepage: www.elsevier.com/locate/fuel

Full Length Article

Fractionation of asphaltenes in *n*-hexane and on adsorption onto $CaCO_3$ and characterization by ESI(+)FT-ICR MS: Part I

Fernanda Endringer Pinto[a], Eliane V. Barros[a], Lilian V. Tose[a], Lindamara M. Souza[a], Luciana A. Terra[b], Ronei J. Poppi[b], Boniek G. Vaz[c], Gessica Vasconcelos[c], Sreedhar Subramanian[d], Sébastien Simon[d], Johan Sjöblom[d], Wanderson Romão[a,e,*]

[a] Federal University of Espírito Santo (UFES), Vitória, ES 29075-910, Brazil
[b] State University of Campinas (UNICAMP), Campinas, SP 13083-970, Brazil
[c] Federal University of Goiás (UFG), Goiânia, GO 74605-220, Brazil
[d] Ugelstad Laboratory, Department of Chemical Engineering, Norwegian University of Science and Technology (NTNU), N-7491 Trondheim, Norway
[e] Federal Institute of Education, Science and Technology of Espírito Santo, Vila Velha, ES 29106-010, Brazil

ARTICLE INFO

Keywords:
Petroleomics
Asphaltenes
ESI-FT-ICR MS
Fractionation
Solubility

ABSTRACT

Two methods of asphaltenes fractionation have been employed to facilitate the characterization of their respective subfractions. The methods are based on step-wise precipitation with different *n*-hexane/crude oil ratios, and on adsorption onto $CaCO_3$. Three subfractions were produced for each method, being named of 3.5 V, 3.5–6 V, and 6–40 V (for the first method); and non-adsorbed (bulk), adsorbed, and irreversibly adsorbed (for the second method). The fractions were characterized by elementary analysis, nuclear magnetic resonance of proton (^{1}H NMR) and by positive ion-mode electrospray Fourier transform ion cyclotron resonance mass spectrometry (ESI(+)FT-ICR MS). The elemental analysis, described in previous work, revealed that the C/H ratio for whole asphaltene and its sub-fractions varied between a narrow range (0.83–0.88) which means they present similar aromaticity or unsaturation. Furthermore, the elemental analysis corroborates with the ^{1}H NMR analysis suggesting that subfraction 6–40 V presented a more aromatic profile than of remaining subfractions, while for the fractionation using $CaCO_3$, this behavior was observed for the adsorbed subfraction. However, a more detailed molecular information was obtained from ESI(+)-FT-ICR MS data, showing that polar compounds species with lower carbon numbers were mainly found for the irreversibly adsorbed subfraction. Besides, the double bond equivalent (DBE) distribution is an important tool to associate the chemical information with solubility parameters, in which, a narrower DBE distribution was observed for irreversibly adsorbed (for fractionation onto $CaCO_3$) and subfraction 3.5 V (fractionation in *n*-hexane) samples, indicating that they are less soluble in hydrocarbons. Also, solubility parameters (δ) were calculated from ESI(+)FT-ICR MS data, where the results indicate that subfractions produced in *n*-hexane have a lower tendency to precipitate in hydrocarbons in relation to subfractions produced onto $CaCO_3$.

1. Introduction

Asphaltene is known to be related to several problems in the oil industry, because of their propensity to flocculate, and precipitate [1,2], causing deposition in the pores of formation rocks, valves, pumps, and refining process [1,3]. These problems have been associated with the highly aromatic asphaltene's components [2]. For this reason, the industry is focused on the study this complex mixture to better understand the composition and behavior of asphaltenes, in order to improve the process of production of crude oil through prevention of deposition of asphaltenes.

Asphaltenes are the most polar fraction of the heavy oil. They are soluble in aromatic solvents (toluene) and insoluble in aliphatic solvents such as heptane [2,4,5]. Concerning their chemical characteristics, as briefly mentioned above, they are composed of a large number of molecules, with polycondensed aromatic rings, high heteroatom content (N, O, and S) and metal compounds such as nickel, vanadium, and iron [2,4–6].

Due to its inherent complexity, the analysis of asphaltenes is a hard and a difficult task, being necessary methods of fractionation and separation of asphaltenes into subfractions with the purpose to facilitate the analysis of such complex feedstock [7]. Asphaltene subfractions are

* Corresponding author at: Federal University of Espírito Santo (UFES), Vitória, ES 29075-910, Brazil.
E-mail address: wandersonromao@gmail.com (W. Romão).

http://dx.doi.org/10.1016/j.fuel.2017.09.028
Received 28 March 2017; Received in revised form 4 September 2017; Accepted 7 September 2017
Available online 23 September 2017

a more uniform sample, regarding composition and physicochemical properties [8]. Generally, these methods use samples of asphaltenes previously precipitated from crude oil with alkanes [8], which is fractionated with a combination of different solvents in different proportions [9–10]. Asphaltene fractionation procedure can also be based on the adsorption properties of asphaltenes onto different surfaces (mineral and metal) [12].

Several examples of asphaltene fractionation are described in the literature. In 1998, Tojima et al. [13] developed a fractionation method using a binary solvent mixture of toluene – heptane (35:65. 25:75. 18:82 v/v) in a reflux condition and were able to recover four fractions (A, B, C, D) of asphaltene by ultracentrifugation. These fractions were characterized by H/C ratio, carbon aromaticity (^{1}H NMR spectroscopy) and average molecular weight (M_w) by vapor pressure osmometry (VPO). Fraction A was classified as heavy asphaltene, being the least soluble, having the lowest H/C ratio and, the most aromatic compared to the other fractions (B, C, and D), which were classified as light fractions.

Following the method developed by Tojima et al. [13], Okhotnikova et al. [14] derived five fractions of asphaltenes. However, they studied only the fraction that precipitated upon minimum and maximum additions of the precipitating agent (65 and 90%, respectively). Fractions were characterized by electron paramagnetic resonance spectroscopy, thermal analysis, calorimetry and atomic force microscopy. The analyses revealed that the fractions presented the same behavior as described by Tojima et al. [13], where the first fraction precipitated had the highest M_w distribution, highest aromaticity factor, lowest H/C ratio and solubility. On the other hand, the last fraction precipitated presented exactly the opposite behavior as the first, being denominated the low M_w fraction.

Trejo et al. [15] also employed this same technique and found the same behavior for the first and subsequently fractions as described in the previous works cited [13,14]. In this study, fractions were characterized by elemental analysis, atomic absorption, VPO aggregated weight and NMR analyses. In another work of Trejo and Ancheyta [16], they also used the binary solvent mixture to fractionate hydrotreated Maya crude oil and characterize the fractions by elemental analysis, atomic absorption and matrix-assisted laser desorption ionization mass spectrometry (MALDI-MS). The fractions presented the same characteristics, as cited in previous studies [13–15], where the first fraction obtained, had a lowest H/C ratio, indicating the presence of aromatic compounds [16].

In 2007, Fossen et al. [17] isolated asphaltene subfractions directly from crude oil by precipitating them by successively increasing *n*-pentane to crude oil ratio. Four fractions of asphaltene were obtained (3:1; 10:1, 15:1, 20:1% v/v of *n*-pentane:crude oil) and characterized by near infrared spectrometry (NIR) and interfacial tensiometry. They concluded that fraction 3:1 was the least soluble and fraction 15:1 was the more soluble in *n*-pentane. In relation to the interfacial tension, the fraction 10:1 showed the highest interfacial activity than the other fractions.

In 2013, Petrova et al. [8] proposed a fractionation scheme where a resin-asphaltene concentrate was precipitated from oil residue that was mixed with acetone in a ratio proportion of 3:1 v/v% (acetone:residue). Subsequently, two fractions (resin–asphaltene concentrate and deasphalted oil) were isolated with *n*-heptane (1:40 v/v) and then, four asphaltenes subfractions were produced from a reflux system filled with a mixture of residue:*n*-heptane:toluene (1:85:1 v/v). These fractions were analyzed by Fourier transform IR spectroscopy (FT-IR), MALDI-MS, and UV spectrophotometry, which the results showed that they exhibited mainly a difference about aromaticity degree and the M_w distribution [8].

In a more recent work, Subramanian et al. [12] proposed a fractionation method based on the adsorption of asphaltene onto calcium carbonate ($CaCO_3$). Three asphaltene fractions were obtained: bulk asphaltene, adsorbed asphaltene and irreversible-adsorbed asphaltene. UV-spectroscopy, elemental analysis, and FT-IR were used to characterize these fractions. These analyses indicated that these fractions were separated with different absorbance's at 1700 cm^{-1}, corresponding to the presence of carbonyl, carboxylic acid or derivative groups, which were more concentrated in the irreversibly adsorbed subfraction. Of all the techniques used to characterize the asphaltene subfractions in the works reported above, few studies have employed the ultrahigh resolution mass spectrometry such as Fourier transform ion cyclotron resonance mass spectrometry (FT-ICR MS) in chemical characterization of asphaltenes subfractions. Therefore, FT- ICR MS will be used to explore the compositional characteristics of asphaltenes subfractions linking their properties to the physical behavior of each fraction.

The "soft ionization" techniques in MS, e.g., electrospray ionization (ESI) and atmospheric pressure photoionization (APPI) are ionization sources of MS most applied in the characterization of asphaltenes [1,18]. The APPI, for instance, has clarified many aspects of asphaltenes fractions [6], such as the confirmation of that asphaltenes are fractions more aromatic than maltenes when establishing the same chain size [19] and, compositional component model [20]. These ionization sources coupled to FT-ICR MS, provide the most extensive information on a molecular level of asphaltenes and complex mixture of petroleum [2,18] since the FT-ICR MS can differentiate thousands of species in a single mass spectrum [2,18]. This behavior is due to the ultra high resolution and accuracy of FT-ICR MS, [21,22] where the molecular formula ($C_cH_hN_nO_oS_s$) can be assigned to each *m/z* detected, thus facilitating, the material classification by heteroatom content and the degree of aromaticity [4,9,23–24].

ESI is particularly efficient in generating acceptable data for polar constituents with high heteroatom content. The combination of positive and negative ESI with FT-ICR MS analysis of asphaltenes was reported by Klein et al. [30], and Pereira et al. [4] Although ESI generates abundant ions from several polar species, substituted hydrocarbon cycloalkanes, and highly aromatic hydrocarbons species usually are not ionized by ESI. However, Molnárné Guricza and Schrader [2] ionized no-polar hydrocarbons and polyaromatic heterocycles species by ESI using appropriated solvents compositions and capillary voltage. Therefore, this source can be more explored to improve the ionization of asphaltene species. Herein, the asphaltene was fractionated using two distinct methodologies: (i) the first, from a crude oil sample as function of volume of *n*-hexane (from 3.5 to 40 V) via partial precipitation of asphaltenes due to a gradual change in the solubility of the medium in which they were dissolved, (ii) and the second, by adsorption onto $CaCO_3$. The asphaltene subfractions produced as well as the whole asphaltene were characterized by ESI(+)FT-ICR MS. These results were compared with aromaticity parameters obtained from elemental analysis and ^{1}H NMR spectrometry measurements.

2. Experimental section

2.1. Samples and reagents

The reagents such as *n*-hexane (VWR, > 97%), anhydrous toluene (Sigma Aldrich, 99.8%), anhydrous tetrahydrofuran (THF) (VWR, > 99.7%), chloroform ($CHCl_3$) (Merck, > 97%), 4 N hydrochloric acid (HCl) and calcium carbonate ($CaCO_3$) (Speciality Minerals Inc., USA) were used in the asphaltene extraction and in production of its subfractions. The 4 N HCl solution was prepared by diluting HCl fuming (Merck, 37%) with purified water. Tetramethylsilane (TMS) and deuterated dichloromethane (CD_2Cl_2) were supplied by Vetec® Química Fina Ltda (Rio de Janeiro- Brazil) and used for ^{1}H NMR analysis. Methanol (99.9%, MeOH), sodium trifluoroacetate (98%, NaTFA) and formic acid (99%, HCOOH) were purchased from Sigma-Aldrich Chemicals (St. Louis USA) whereas toluene (98%,) was purchased by Vetec® Química Fina Ltda (Rio de Janeiro-Brazil).

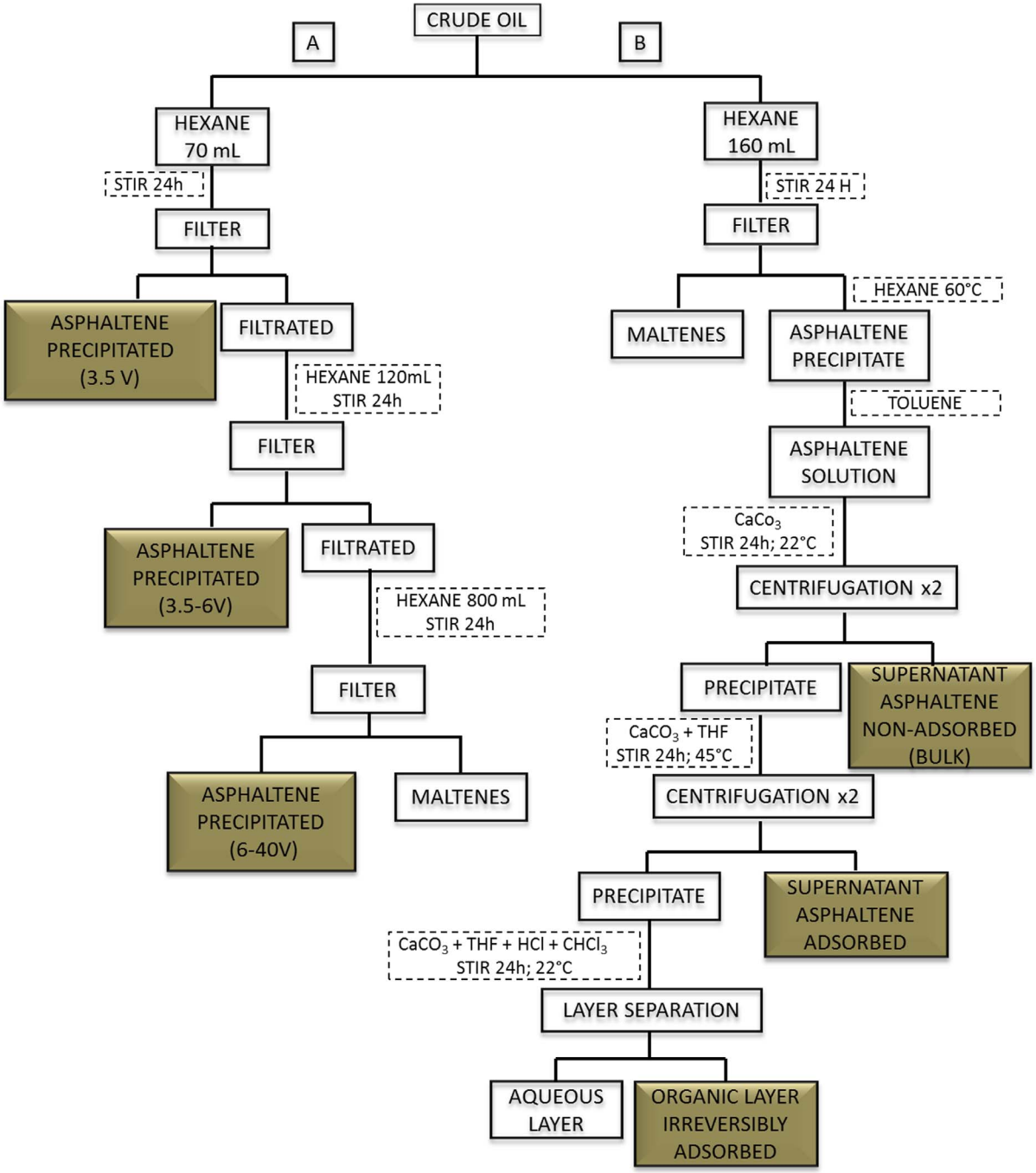

Fig. 1. Scheme of asphaltenes extraction from crude oil. Letter A represents the extraction and fractionation of asphaltene in different volumes of *n*-hexane and letter B represents the extraction and fractionation of asphaltene in $CaCO_3$.

2.2. Asphaltene extraction and fractionation in n-hexane

The asphaltene subfractions analyzed in this work were fractionated and provided by Subramanian et al. [33] The crude oil was submitted to an extraction procedure to obtain different asphaltenes subfractions. An overall scheme of the fractionation can be view in Fig. 1(A), where three different volume ranges of *n*-hexane (3.5 V; from 3.5 to 6 V and from 6 to 40 V) were used to obtain the subfractions of asphaltenes. Briefly, the crude oil (20 g) was put in contact with *n*-hexane (70 mL, equivalent to 3.5 mL/g crude oil) and stirred for 24 h. The solution was then filtering under vacuum using a 0.45 μm (Sartorius Stedium) membrane filter, subsequently washed with *n*-hexane (50 mL). The first fraction of asphaltene (subfraction 3.5 V) was obtained from the precipitated with a yield of 27.4% (Table 1). After 120 mL (6 V) of *n*-hexane was added to the filtrated, this solution was then submitted to agitation for 24 h. Posteriorly, it was filtered and washed with *n*-hexane, obtaining the second asphaltene fraction (subfraction 3.5–6 V) with a yield of 32.3% (Table 1). After, 800 mL (40 V) of *n*-hexane was added to the filtrate, stirred for 24 h and subsequently was filtered and washed as described above. The last asphaltene fraction was obtained (subfraction 6–40 V) with a yield of 40.3% (Table 1). All subfractions obtained were dried under nitrogen at room temperature [33].

2.3. Asphaltene extraction and fractionation in $CaCO_3$

The asphaltene subfractions analyzed in this work were fractionated

Table 1
Elemental analysis of whole asphaltenes and subfractions obtained in the fractionation with *n*-hexane in different volumes and fractionation onto $CaCO_3$ are taken from Subramanian et al. [33,12].

Elements	Whole Asphaltene	Subfractions					
		3.5 V	3.5–6 V	6–40 V	Non-adsorbed (Bulk)	Adsorbed	Irreversibly adsorbed
C (wt%)	85.6	82.3	86.1	86.2	85.7	84.3	83.2
H (wt%)	8.17	7.95	8.21	8.16	8.12	8.00	8.30
N (wt%)	1.32	1.27	1.36	1.35	1.20	1.40	1.35
O (wt%)	1.85	2.84	1.73	1.79	2.33	3.27	4.22
S (wt%)	1.96	2.09	2.13	2.12	1.91	2.28	2.14
Total	98.90	96.45	99.53	99.62	99.26	99.25	99.41
C/H ratio	0.873	0.863	0.874	0.880	0.880	0.878	0.837
Yield (mass%)	–	27.4 ± 0.8	32.3 ± 0.9	40.3 ± 1.2	51.2 ± 0.5	29.9 ± 1.4	17.1 ± 0.6

and provided by Subramanian et al. [12]. Asphaltene was extracted from crude oil by precipitation in *n*-hexane and then fractionated into subfraction based on the adsorption of asphaltene onto $CaCO_3$. The $CaCO_3$ compound was selected as adsorbent due to the fact it imitates typical calcium carbonate reservoirs. An overall scheme of fractionation can be view in Fig. 1(B). Briefly, 160 mL portion of hexane was added to 4 g of crude oil sample (40 mL g^{-1} of oil) and stirred for 24 h at room temperature. The solution was then filtering using a 45 μm (Sartorius Stedium) membrane filter, separating the precipitated asphaltene from the maltenes. This precipitated asphaltene, named the whole asphaltene, was washed with hexane and dried. Subsequently, whole asphaltene (1.5 g) was solubilized in toluene (375 mL) and sonicated for 30 min, resulting in a 4 g mL^{-1} asphaltene solution concentration. To this asphaltene solution was added $CaCO_3$ (41.4 g). This mixture was stirred for 24 h at 22 °C. After it was centrifuged (4000 rpm) for 20 min., filtered and the non-adsorbed asphaltene subfraction (supernatant) was obtained. Subsequently, THF (375 ml) was added to $CaCO_3$, stirred for 24 h at 45 °C and then centrifuged (4000 rpm) for 20 min. The supernatant was recovered, filtered and named adsorbed subfraction. To obtain the subfraction remaining on the surface of $CaCO_3$, 750 mL of a solution containing THF:$CHCl_3$ (50:50 v/v) was added to $CaCO_3$. Posteriorly, 750 mL of 4 N HCl solution was added slowly to the mixture and stirred at room temperature for 3 h. Afterwards, the organic and aqueous layer was separated using a separating funnel. The organic layer was labeled irreversibly adsorbed subfraction [12].

2.4. Chemical characterization

2.4.1. Elemental analysis

The details of the elemental analysis procedure are reported elsewhere for the samples obtained in the fractionation onto $CaCO_3$ and the fractionation in n-hexane [12,33]. The contents of carbon (C), hydrogen (H), nitrogen (N), oxygen (O) and sulfur (S) of the crude oil, of the asphaltene and subfractions, were determined by Laboratory SGS Multilab (Evry, France).

2.4.1.1. ^1H nuclear magnetic resonance (^1H NMR). To characterize the content of aromatic and aliphatic hydrogens, NMR spectroscopy experiments were performed using a Varian 400 MHz spectrometer, operating at 9.4 T using 5 mm broadband $^1H/X/D$ probe at 26 °C and 45° pulse. The experiments were performed using a spectral window of 6410.3 Hz and a relaxation delay of 1.16 s and 128 scans. Approximately 20 mg of each sample was diluted in 0.7 mL of CD_2Cl_2. TMS was used to reference the chemical shifts. The degree of aromaticity (%) of asphaltene and its subfractions were determined through the integration of spectra from 9.0 to 6.0 ppm (for aromatic hydrogen) and from 4.0 to 0.0 ppm (for aliphatic hydrogen). This procedure was analogous to the one described by da Silva Oliveira et al. [32] and Nascimento et al. [34].

2.4.2. FT-ICR MS

FT-ICR MS [25–29] analysis was performed using a 9.4 T Q-FT-ICR MS hybrid (Solarix, Bruker Daltonics Bremen, Germany) equipped with commercially available ESI source (Bruker Daltonics) set to operate over *m/z* 200–1200. FT-ICR mass spectra of whole asphaltene and its respective subfractions were acquired using positive-ion ionization mode for ESI, ESI(+).

All samples were diluted to 0.5 mg mL^{-1} for ESI (+) in 50:50 (v/v) toluene/methanol containing 0.1% v/v of HCOOH. To ensure the solubility of all samples, they were sonicated for 5 min, and after were directly infused at a flow rate of 10 μL min^{-1} for ESI [4,18,34–35,36].

The ESI(+) source conditions were as follows: nebulizer gas pressure of 1.4 bar, capillary voltage of −3.5 kV, and transfer capillary temperature of 250 °C. The ions were accumulated in the hexapolar collision cell with time of 0.1 s followed by transport to the ICR cell through the multipole ion guide system (another hexapole). The front and back trapping voltages in the ICR cell were 60 V and - 55 V, respectively, for ESI(+).

Each spectrum was acquired by accumulating 200 scans of time-domain transient signals in 4 mega-point time domain data sets. All mass spectra were externally calibrated using a NaTFA solution 0.05 mg mL^{-1} (*m/z* from 200 to 1200) [4,18] and posteriorly were internally recalibrated using a set of the most abundant homologous alkylated compounds for each sample. A resolving power, $m/\Delta m_{50\%}$ = 465,000–610,000 (in which $\Delta m_{50\%}$ is the full peak width at the half-maximum peak height of *m/z* 400) and a mass accuracy of < 1 ppm provided the unambiguous molecular formula assignments for singly charged molecular ions.

The mass spectra were acquired and processed using a custom algorithm developed specifically for petroleum data processing, Composer software (Sierra Analytics, Modesto, CA, USA) [31]. Elemental compositions of the compounds were determined by measuring the *m/z* values, and the M_w is obtained based on the centered value of Gaussian profile. Heteroatomic-containing compounds profile, double bond equivalent (DBE) versus carbon number (CN), and van Krevelen diagrams were constructed to visualize and interpret the MS data [4,18]. The unsaturation level of each compound can be deduced directly from its DBE value according to Eq. (1):

$$DBE = c - h/2 + n/2 + 1 \quad (1)$$

where *c*, *h*, and *n* are the numbers of carbon, hydrogen, and nitrogen atoms, respectively, in the molecular formula.

Solubility parameters were also obtained based on the work of Rogel et al. [9], where they evaluated the characteristics of asphaltene, linking chemical composition to the solubility and thermal behavior. According to their work, solubility parameters were calculated by using the third rule that correlates density with solubility parameter for hydrocarbon molecules (Eq. (2)) [37].

$$\delta = 17.347\rho + 2.904 \quad (2)$$

where δ is the solubility parameter ($MPa^{0.5}$), and ρ is the density (g/

Table 2
^{1}H NMR analysis of whole asphaltenes and subfractions obtained in the fractionation with *n*-hexane and fractionation onto $CaCO_3$.

Chemical shift (ppm)	Whole asphaltene	Subfractions in *n*-hexane			Subfractions onto $CaCO_3$		
		3.5 V	3.5–6 V	6–40 V	Non-adsorbed	Adsorbed	Irreversibly adsorbed
% H_{ar} (6.0–9.0)	11.9	11.2	12.4	11.8	9.5	10.6	8.8
% H_{alq} (0.5–4.0)	88.1	88.8	87.6	88.2	90.5	89.4	91.2
% H_γ (0.5–1.0)	17.3	17.4	17.0	17.5	14.6	17.9	19.0
% H_β (1.0–2.0)	51.8	51.7	51.2	51.7	59.4	53.3	53.4
% H_α (2.0–4.0)	19.0	19.7	19.5	19.1	16.4	18.2	18.8

.

cm^3). The density values were calculated according to Eq. (3), where H represents the hydrogen content (wt%).

$$\rho = -0.064\ H + 1.6793 \quad (3)$$

A correction of solid densities was performed by applying Eq. (4), because the reference for the solubility parameter is a liquid state, being necessary applying a ratio between the solid density and liquid density at triple point [9]:

$$\rho_s/\rho_L = 1.17 \quad (4)$$

3. Results and discussion

3.1. Elemental analysis and ^{1}H -NMR

Whole asphaltene and its subfractions obtained from fractionation by *n*-hexane and fractionation onto $CaCO_3$ were characterized by elemental analysis (C, H, N, S, and O) by Subramanian et al. [12,33] and the results are summarized in Table 1. ^{1}H NMR results performed by our group are described in Table 2. Regarding the elemental contents (Table 1), subfractions 3.5–6 V and 6–40 V presented higher values of carbon and hydrogen contents (C = 86.1 and C = 86.2 wt%, and H = 8.21 and H = 8.16 wt%, respectively). Note also that a subtle change of C/H ratio values for asphaltenes subfractions can be observed, ranging from 0.863 to 0.880, presenting the following order: subfraction 3.5 V < whole asphaltene < subfraction 3.5–6 V < subfraction 6–40 V. The whole asphaltene has similar C/H ratio when compared to intermediary subfraction, subfraction 3.5–6 V. In general, the aromaticity degree or unsaturation level of asphaltenes precipitated increases as a function of the volume of *n*-hexane added in crude oil, where the values obtained are similar to those reported in the literature [38,39].

Among the asphaltenes subfractions, the subfraction 3.5 V shows a lower C/H ratio indicating that it has a higher aliphatic character compared to the remaining subfractions. This fact can be corroborated by the results of ^{1}H NMR analysis (Table 2), where lower aromatic hydrogen content is observed for this subfraction. Note also that an increase of oxygen content is observed for this same fraction, ranging from 1.85 wt% (for the whole asphaltene) to 2.84 wt% (for the subfraction 3.5 V), Table 1. However, this value decreases approximately 40% when compared to remaining subfractions (3.5–6 V and 6–40 V). It can also be observed that the nitrogen and sulfur contents (Table 1) in all the asphaltene subfractions are very similar. Therefore, if a higher C/H ratio implies in a greater number of fused aromatic rings, we can conclude that the subfractions 3.5–6 V and 6–40 V were highly enriched in aromatic carbons while the fraction 3.5 V was diminished.

In 2003, Spiecker et al. [39] analyzed asphaltene samples obtained from different crude oils (Arab Heavy, B6, Canadon Seco, and Hondo) using mixtures of heptane and toluene (70:30 and 60:40 v/v%). In this case, the precipitated fractions (enriched with O, N, Ni, and V) were more aromatic than whole asphaltene samples. In 2004, Östlund et al. [11] also used a procedure that caused the partial precipitation of asphaltenes due to a gradual change in the solubility of the medium. Methylene chloride was used as polar solvent and n-pentane as a flocculant. The subfraction obtained was more aromatic in relation to unfractionated asphaltene, and contains asphaltene compounds that had the strongest tendency to flocculate. In this work, the subfraction 6–40 V can have chemical properties similar to previously described, since that it is clear that has higher C/H ratio than the whole asphaltene. The ^{1}H NMR spectrum can be visualized in Fig. 1S.

The results of elemental analysis of subfractions obtained from the fractionation onto $CaCO_3$ (Table 1) [12] reveal that the subfractions presented similar profile since their C/H ratio varied between a narrow range (0.837–0.880). However, a lower value of C/H ratio was observed for the irreversibly adsorbed subfraction when compared to the remaining subfractions, indicating a more aliphatic profile for this fraction [12]. This decrease in C/H ratio could be due to the increase of oxygen content, attributed to the contamination by $CaCO_3$ [12]. The C/H ratio obeys the following order for whole asphaltene and its subfraction samples: irreversibly adsorbed < whole asphaltene ~ adsorbed < non-adsorbed. The ^{1}H NMR results corroborate with this fact (Table 2), where lower aromatic hydrogen content is observed for irreversibly adsorbed subfraction. The results suggest that the irreversible adsorption onto $CaCO_3$ particles is preferential to fractions with less aromatic hydrogen content [34]. The ^{1}H NMR spectrum can be visualized in Fig. 2S.

3.2. FT-ICR MS

Many studies have shown that the FT-ICR MS analysis will discriminate the chemical profile of the asphaltenes, where an enhancement or suppression of the compounds classes can occur depending on the ionization method applied [4,40–41,42]. The ESI source readily ionizes polar compounds containing nitrogen and oxygen atom. However, it is more challenge to ionize low polar or nonpolar components [4,42].

Fig. 2a–h displays the ESI(+)FT-ICR mass spectra of whole asphaltenes and subfractions obtained by fractionation in different volumes of *n*-hexane (Fig. 2a–d) and by fractionation onto $CaCO_3$ (Fig. 2e–h). In general, ESI(+)FT-ICR mass spectra (Fig. 2) shows broadband profiles from *m/z* 200–900 with average molecular weight distribution (M_w) centered at approximately *m/z* 493 for whole asphaltene (Fig. 2a and e). The M_w of subfractions obtained from the fractionation in *n*-hexane (Fig. 2b–d) is centered at approximately *m/z* 534 (2b), 528 (2c), and 508 (2d) (for samples 3.5 V, 3.5–6 V, and 6–40 V, respectively). Mass spectra of samples obtained from the fractionation onto $CaCO_3$ (Fig. 2f–h) presented M_w centered at approximately *m/z* 508 (2f), 399 (2g), and 442 (2h) (bulk, adsorbed and irreversibly adsorbed subfractions, respectively). M_w values obey the following order for the fractionation in *n*-hexane: subfraction 3.5 V > subfraction 3.5–6 V > subfraction 6–40 V (Fig. 2b–d), whereas the fractionation onto $CaCO_3$ (Fig. 2f–h), it decreases in the following order: non-adsorbed (bulk) > irreversibly adsorbed > adsorbed subfraction.

Heteroatom class distribution for whole asphaltene and subfractions are shown in Fig. 3a–b. The most abundant classes detected was the N

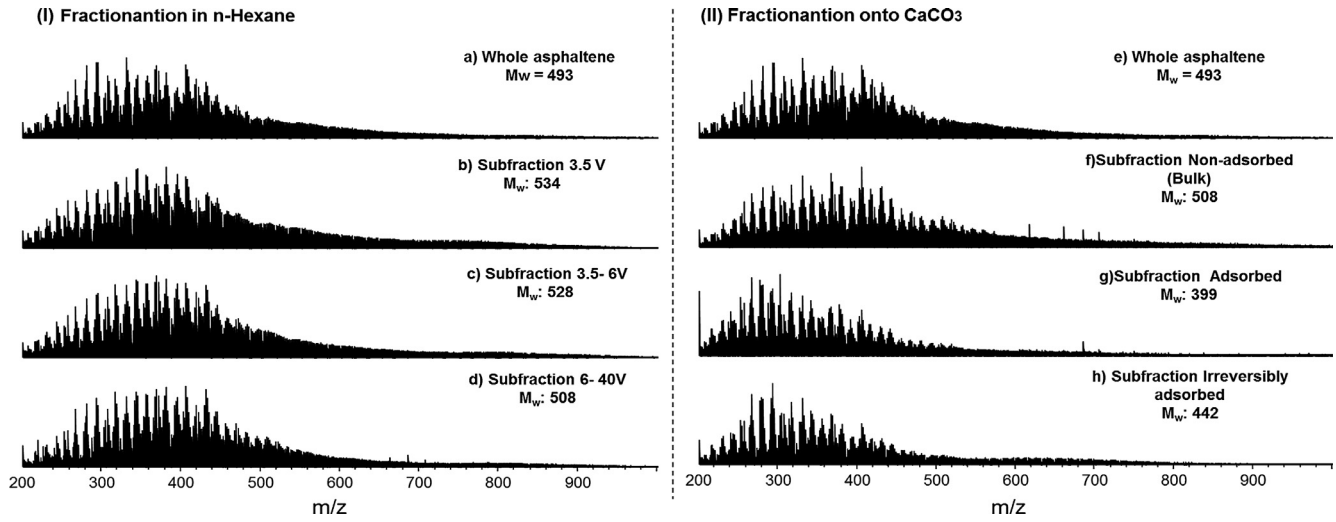

Fig. 2. ESI(+)FT-ICR MS mass spectra of whole asphaltene and its subfractions obtained by fractionation in different volumes of *n*-hexane (I) and onto calcium carbonate (II).

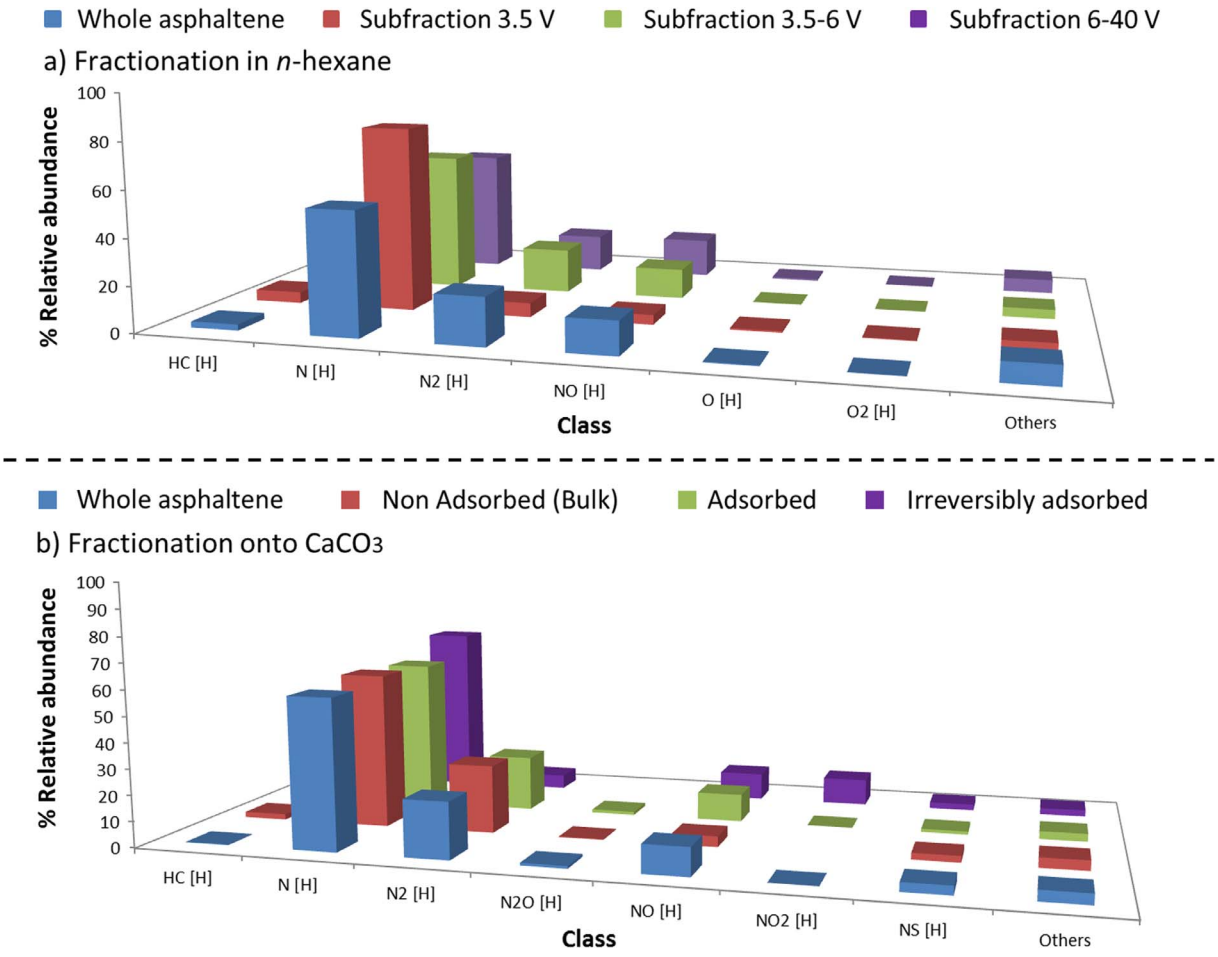

Fig. 3. Class distribution generated from ESI(+)FT-ICR MS data for whole asphaltene and subfractions obtained by fractionation in *n*-hexane (a) and fractionation onto $CaCO_3$ (b).

[H] class* following by N2[H], NO[H] and HC[H] classes. The relative abundances in the compounds classes between subfractions presented small differences. For example, from subfractions 3.5 V to subfraction 6–40 V (Fig. 3a), N[H] class decreases (80% to 55%), whereas N2[H] class is increased (6%–16%). An opposite behavior is observed in the subfractions obtained by the adsorption process (Fig. 3b). From non-adsorbed subfraction to irreversibly adsorbed subfraction, class N[H] is increasing (60%–67%), while class N2[H] is decreasing (26% to 6%). The NO[H] class increased between all fractions. Although irreversibly adsorbed subfraction presented a higher percentage of oxygen, these compounds were not ionized in the ESI(+), mainly because ESI(+) facilitates the detection of basic compounds, thus suppressing, the ionization of more acidic species, such as O and O_2 classes and some mixed classes (NO and N_2O classes, etc.) [43,44].

* CLASS[H] is used to design ions classes identified in protonated or deprotonated form

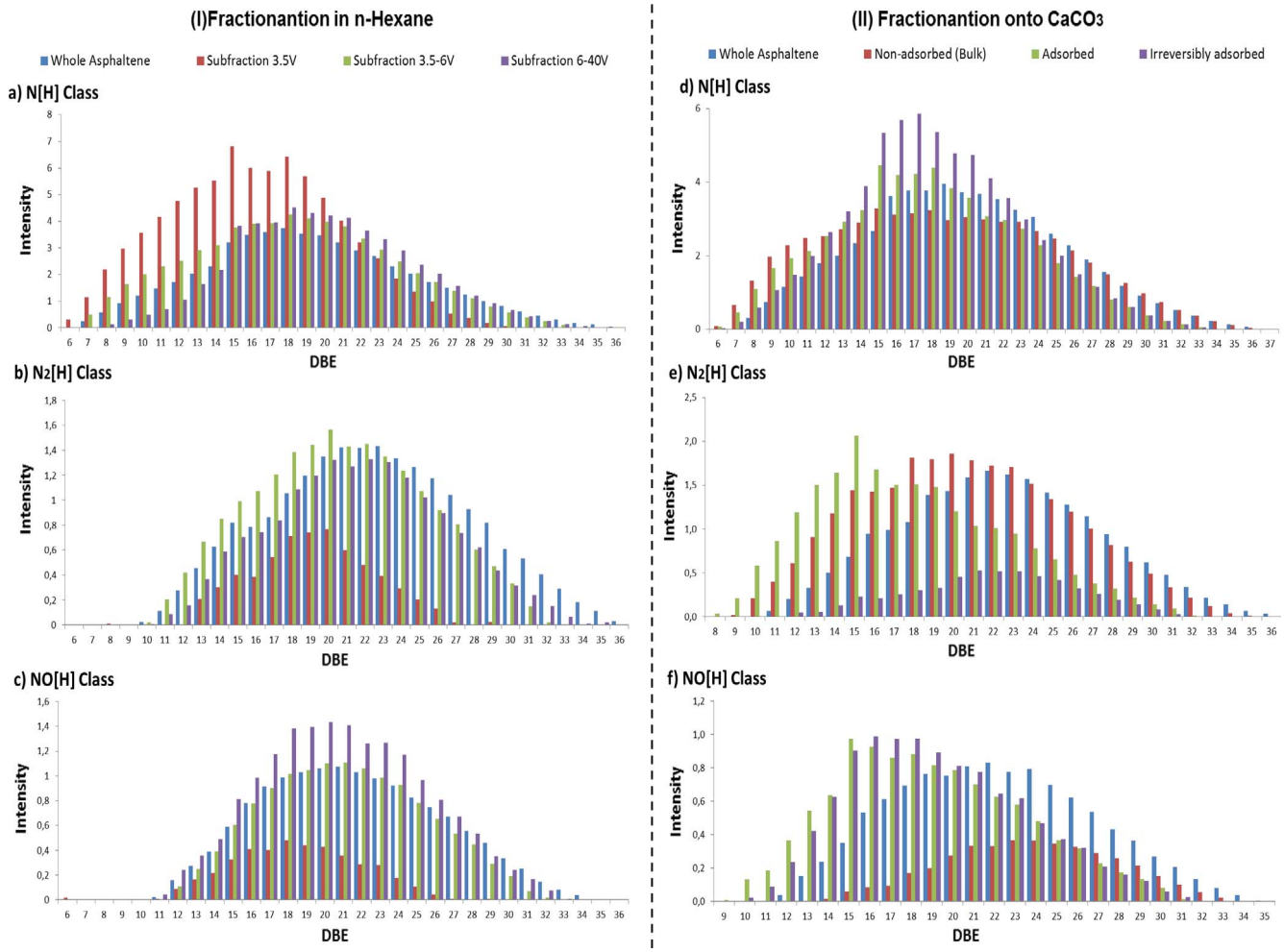

Fig. 4. DBE relative abundance distribution for N[H] (a and d), N_2[H] (b and e) and NO[H] (c and f) classes for the whole asphaltene and its subfractions obtained by fractionation in *n*-hexane (I) and fractionation onto $CaCO_3$ (II).

The number of polar compounds species (obtained from the sum of assigned molecular formulas) observed for the whole asphaltene was of 2914; whereas for subfractions obtained by fractionation in different volumes of *n*-hexane, the values found were 3458, 3572, and 3411 for samples 3.5 V, 3.5–6 V, and 6–40 V, respectively. For subfractions obtained by fractionation onto $CaCO_3$, the number of assigned polar species were 2494, 1598, and 1614 for non-adsorbed (bulk), adsorbed, and irreversibly adsorbed subfractions, respectively. By the number of assigned molecular formula for each sample, we could say that sample 3.5–6 V, and non-adsorbed subfractions present the mostly polar profile. However, analyzing the DBE *vs* carbon number (CN) plots (Fig. 5c and d), we can conclude that the irreversibly adsorbed subfraction presented a higher intensity of molecules with lower carbon numbers than the other fractions. A smaller chain would lead to a higher polarity. We can also note in the van Krevelen plot for the N_xO_y class (Fig. 6p) of irreversibly adsorbed subfraction that exist higher values of N/C ratio for the NO_2 class, indicating a greater amount of heteroatom by carbon, what could also be attributed to a higher polarity of the irreversibly adsorbed subfraction, thus suggesting, that this subfraction is the most polar subfraction among the two fractionation methods studied.

Fig. 4a–f displays the DBE relative abundance distribution of N[H], N2[H] and NO[H] classes of whole asphaltene and its subfractions obtained by the two different methods of fractionation (in *n*-hexane, 4a–c, and onto $CaCO_3$, 4d–f). DBE distribution for the N[H] class (Fig. 4a) for subfraction 3.5–6 V and subfraction 6–40 V presented a shift to higher DBE when compared with subfraction 3.5 V, exhibiting DBE distribution ranging from 6 to 36, having abundance maximum of DBE centered on average at 18. For N2[H] (Fig. 4b) and NO[H] (Fig. 4c) classes, a similar behavior is observed. From this, it can be inferred that these two subfractions presented a more aromatic profile than subfraction 3.5 V. These results are in good agreement to Tables 1 and 2, where lower C/H ratio, N content, and H_{ar} content values were reported for subfraction 3.5 V, being, therefore, classified as less aromatic.

Fig. 4d–f exhibits DBE distribution for whole asphaltene and subfractions obtained by fractionation onto $CaCO_3$. DBE distribution for the N[H] class (Fig. 4d) for whole asphaltene and non-adsorbed subfraction presents a similar and wider DBE distribution, changing from 6 to 36, with abundance maximum centered on DBE = 18–19. On the other hand, adsorbed and irreversibly adsorbed subfractions have similar profile between themselves, displaying a shorter DBE distribution ranging from 6 to 32, with abundance maximum centered on average at DBE = 15–18. For the N_2[H] class (Fig. 4e), DBE distribution differs significantly between subfractions, where irreversibly adsorbed subfraction presented the lowest intensity of N_2[H] class. Observing the DBE distribution for the NO[H] class (Fig. 4f), it is noted that adsorbed and irreversibly adsorbed subfractions exhibit similar profile, whereas whole asphaltene and non-adsorbed subfractions display a very distinguished profile between them.

The DBE and CN distribution have been associated with solubility parameters in hydrocarbons as reported in a study of Rogel and Witt [45], where they used the data generated by APPI-FT-ICR MS to evaluate the effect of solubility parameter on the fractionation of typical

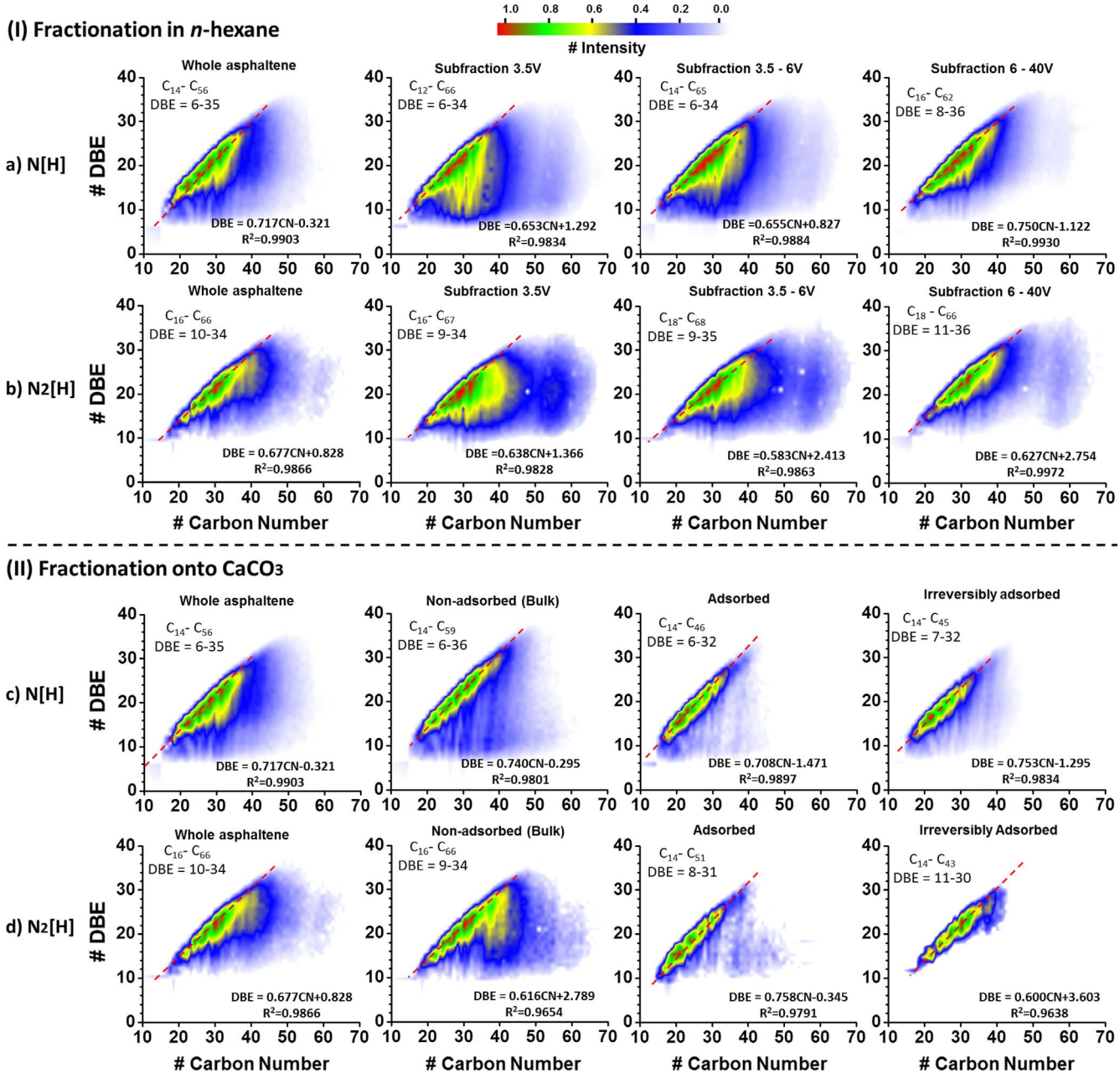

Fig. 5. DBE vs carbon number plots for the N[H] (a and c) and N_2[H] (b and d) classes for whole asphaltene and its subfractions obtained by the fractionation in *n*-hexane (I) and onto $CaCO_3$ (II).

crude oil sample in function of its molecular distribution. They notice that when DBE shifts to higher values or if its distribution became narrow, the fractions became less soluble in hydrocarbons. When analyzed the data of Fig. 4a–b and d–e (N[H] and N_2[H] classes), a narrower DBE distribution is mainly observed for irreversibly adsorbed and adsorbed subfractions (for fractionation onto $CaCO_3$) and subfraction 3.5 (fractionation in *n*-hexane) samples [45], thus indicating, that they have lower solubility in hydrocarbon solvents. The DBE distribution range among the samples can also be better visualized when the DBE data are normalized and fitted as shown in Fig. 4S.

DBE *vs* CN plots can also be used to evaluate the degree of aromaticity [21,46]. Fig. 5 illustrates the most abundant classes (N[H] and N_2[H]), detected by ESI(+) source, for whole asphaltene and its subfractions. As it could be seen for the most samples, that the DBE distribution for the N[H] class, Fig. 5a, ranges from DBE = 6 to 36 and CN between C_{12} and C_{66}. However, subfraction 6–40 V displays a highly aromatic and shorter DBE distribution, containing DBE and CN ranging from 8 to 36 and C_{16} to C_{62}, respectively. The same behavior was noticed in the N_2[H] (Fig. 5b) and NO[H] classes (Fig. 3SI). This fact can be better seen by the DBE *vs* intensity curves for the most abundant classes (Fig. 4a–c), where a clear shift to higher DBE can be seen for the subfraction 6–40 V (Fig. 4a–c), implying that it has a more aromatic profile than the remained subfractions [47].

Analyzing now the DBE *vs* CN plots for the fractionation onto $CaCO_3$, Fig. 5c shows that the N[H] class has a similar profile between whole asphaltene and non-adsorbed subfraction, with DBE distribution ranging from DBE = 6 to 36 and CN from C_{14} to C_{59}. On the other hand, adsorbed and irreversibly adsorbed subfractions also presented similar profiles between themselves, having DBE distribution ranging from DBE = 6 to 32 and CN ranging from C_{14} to C_{46}, thus presenting, a narrow distribution of CN in comparison to the whole asphaltene and non-adsorbed subfraction. Similar behavior was observed for other

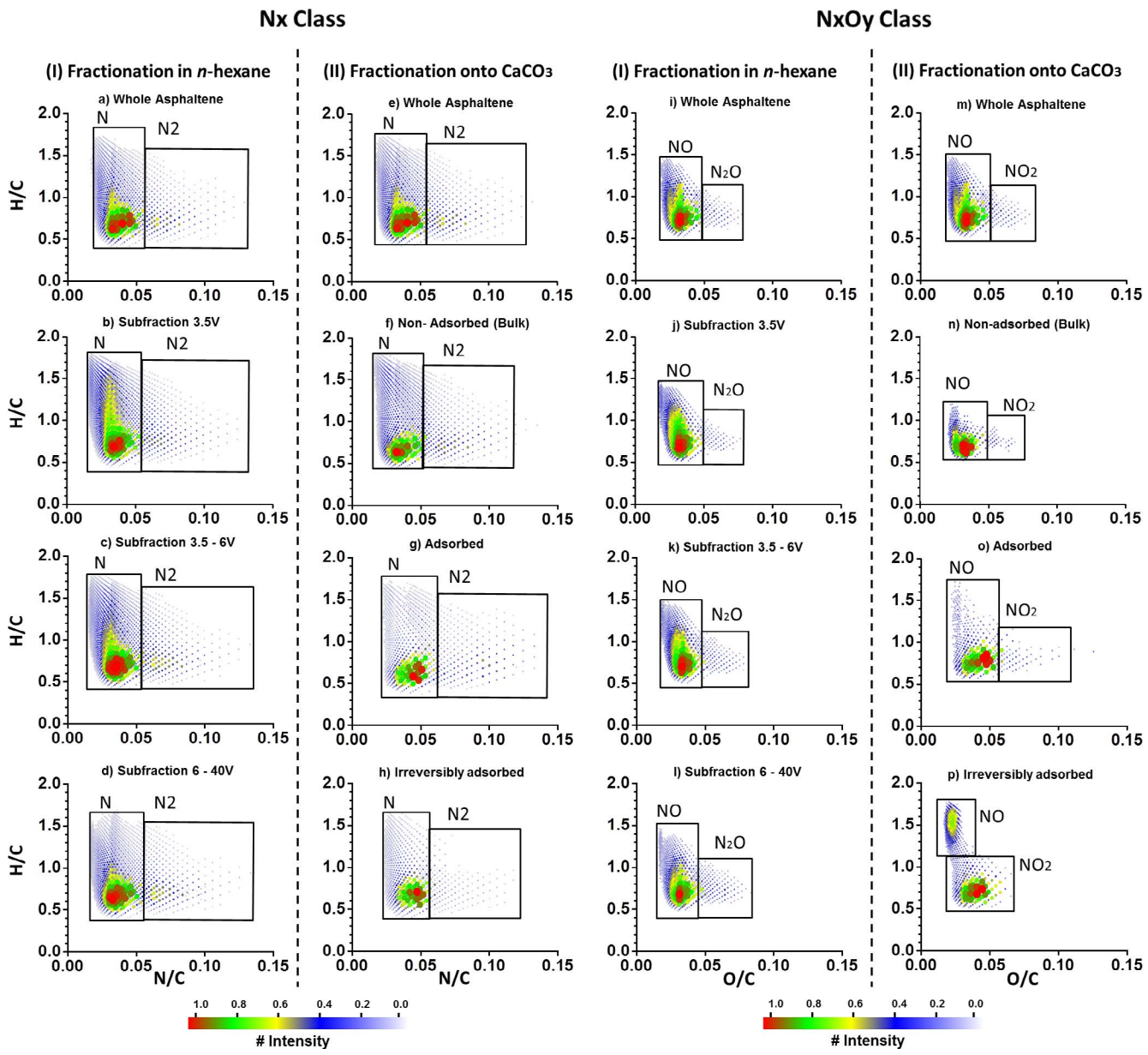

Fig. 6. van Krevelen diagrams for N_x and N_xO_y containing species generated from ESI(+) FT-ICR MS data of whole asphaltene and its respective subfractions obtained by the fractionation in *n*-hexane (I) and onto $CaCO_3$ (II).

classes (N_2[H] (Fig. 5d) and NO[H] classes (Fig. 3SII)).

To determine the aromatic degree, the concept of the planar slope was applied. A diagonal line connecting maximum DBE values for each carbon number was drawn, and the aromatic degree was obtained from the slopes of the lines through the angular coefficient of the linear regression equation, where higher coefficient implied higher aromaticity degree. The lines were calculated by linear regression for N[H] and N_2[H] classes and are shown in Fig. 5. It is comprehended that the inclination of the line increases in function of an increase in H_{ar} values [4,19]. The results show that for N[H], for the subfractions obtained from fractionation with *n*-hexane (Fig. 5a), the slope decreased in the consecutive order: 6–40 V > whole asphaltene > 3.5–6 V > 3.5 V. Thereby similar to the results of elemental analysis and ^{1}H NMR spectroscopy (Tables 1 and 2, respectively). For the subfractions obtained from fractionation onto $CaCO_3$, the slope of N[H] class (Fig. 5c) decreased in the following order: irreversibly adsorbed > non-adsorbed > whole asphaltene > adsorbed.

The van Krevelen diagram can also help elucidate the molecular composition of asphaltenes. This diagram was first created to study coal [48], but since then have been applied in the study of many feedstocks [4,45,49,50]. The van Krevelen diagram consists of *iso*-abundance contoured plots in function of molar ratio of H/C and heteroatom class/C ratio, resulting in a plot where each compound has a specific location on the diagram [4,50] and this way allows the visual separation of heteroatom classes, DBE types and alkylation patterns [4,18].

Fig. 6 illustrates the van Krevelen diagram of the N_x and N_xO_y classes detected during ESI(+)FT-ICR MS analysis. Fig. 6a–d displays the N_x profile of N_1 and N_2 classes for whole asphaltene and subfractions obtained in the fractionation in *n*-hexane. Samples show a similar H/C ratio for the N_1 class, ranging from 0.4 to 1.8. Subfraction 6–40 V (Fig. 6d) has the most abundant species ranging from 0.5 to 1.0, whereas for subfraction 3.5 V (Fig. 6b), it ranges from 0.5 to 1.5. The shift to a lower H/C ratio of subfraction 6–40V suggests that this subfraction has more aromatic compounds than the other samples, because, as the H/C ratio decreases, the number of ring plus double bond increases [46]. The N_2 class was detected in lower amplitude, with an

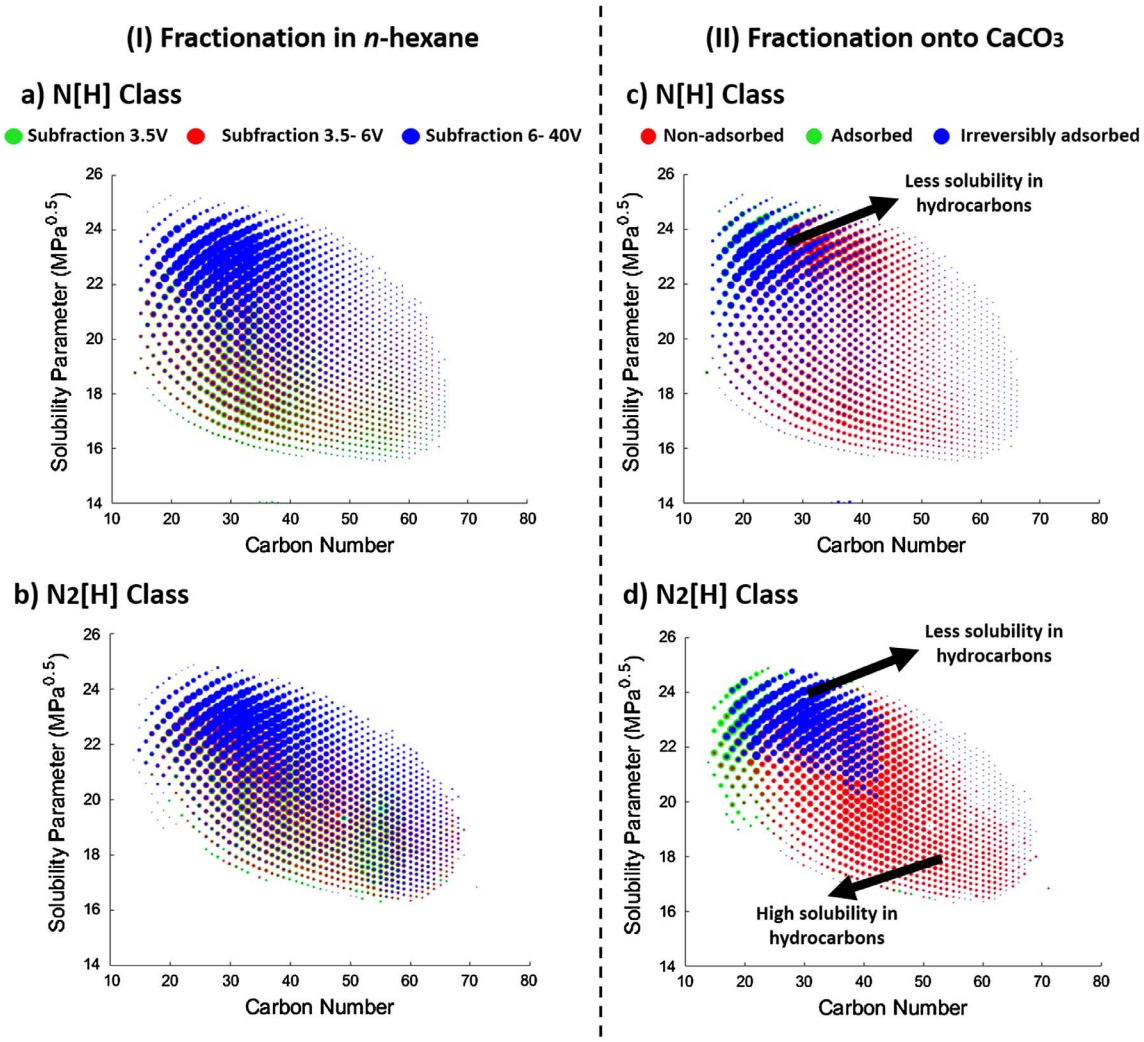

Fig. 7. Solubility parameter *versus* carbon number plots for N[H] and N_2[H] classes for whole asphaltene and subfractions obtained by the fractionation in *n*-hexane (I) and onto $CaCO_3$ (II).

H/C ratio ranging from 0.5 to 1.5.

For samples obtained in the fractionation onto $CaCO_3$ (Fig. 6e–h), the N_x profile shows, for N[H] class, an H/C ratio similar to the samples fractionated in *n*-hexane, ranging from 0.4 to 1.8. However, the most abundant compounds (represented by green, yellow and red dots) presents a shift to lower H/C ratio range, 0.5–0.9. It is also noticeable that between the subfractions (Fig. 6e–h) a decrease of molecules with lower DBE is observed from the whole asphaltene to irreversibly adsorbed subfraction, indicating that the last two subfractions (adsorbed and irreversibly adsorbed, Fig. 6g–h) have fewer compounds with lower DBEs. The N_2[H] class presented similar behavior as the subfractions obtained from fractionation in *n*-hexane (Fig. 6a–d).

In Fig. 6i–p, the van Krevelen graphic for the N_xO_y profile for all samples is shown. The NO class (Fig. 6i–j) was the most abundant class detected in the subfractions, with H/C ratio ranging from 0.5 to 1.5. Note that the NO[H] class presented similar behavior as the N[H] class. Subfraction 6–40V (Fig. 6l) had the most abundant species ranging from 0.5 to 1.0, whereas for subfraction 3.5V (Fig. 6j) it ranges from 0.5 to 1.25. The lower amplitude for the N2O class was observed for all samples, with H/C ratio varying from 0.6 to 1.1.

Fig. 6m–p displays the compounds distribution for NO and NO_2 for samples obtained from fractionation onto $CaCO_3$, where a great difference of the H/C ratio and the range of samples is now reported. Note that the irreversibly adsorbed subfraction resented a higher H/C ratio, indicating that the species containing NO atoms have a lower number of rings plus double bonds. On the other hand, the species present in NO_2 class are highly aromatic, Fig. 6p. In general, it is noticed that the subfractions produced using $CaCO_3$ adsorbent, exhibit a more distinct molecular behavior in relation to its original sample, whole asphaltene [6,12,51].

Solubility parameter distribution graphics as a function of the size of the molecule for N [H] and N_2 [H] classes were built using Eqs. (2) and (3) (Fig. 7). As mentioned before, asphaltenes that have higher hydrogen deficiency (i.e., higher DBE average values), have higher solubility parameters [6,9,50]. In Fig. 7, it can be seen that these asphaltenes with higher solubility parameters, which are less soluble in hydrocarbons, are located on the upper level of the graphic and are associated with aromatic molecules [6]. While asphaltenes that are located in the lower level of the graphic have lower solubility parameters, being more soluble in hydrocarbons can be associated to linear alkanes [6]. The average solubility parameters values were between 16 and 25 $MPa^{0.5}$, agreeing with the values reported in the literature [6].

Fig. 7a shows the solubility parameter of the N[H] class in the subfractions obtained from the fractionation in *n*-hexane. An overlapping of the N classes between the subfractions is observed. In the work of Rogel et al. [9], it is stated that higher overlapping in the solubility/carbon number space of the same classes between the fractions indicates a lower tendency to precipitate, and therefore, similar chemical properties. This overlapping of solubility parameter distribution for the same class can be better visualized in the two-dimensional

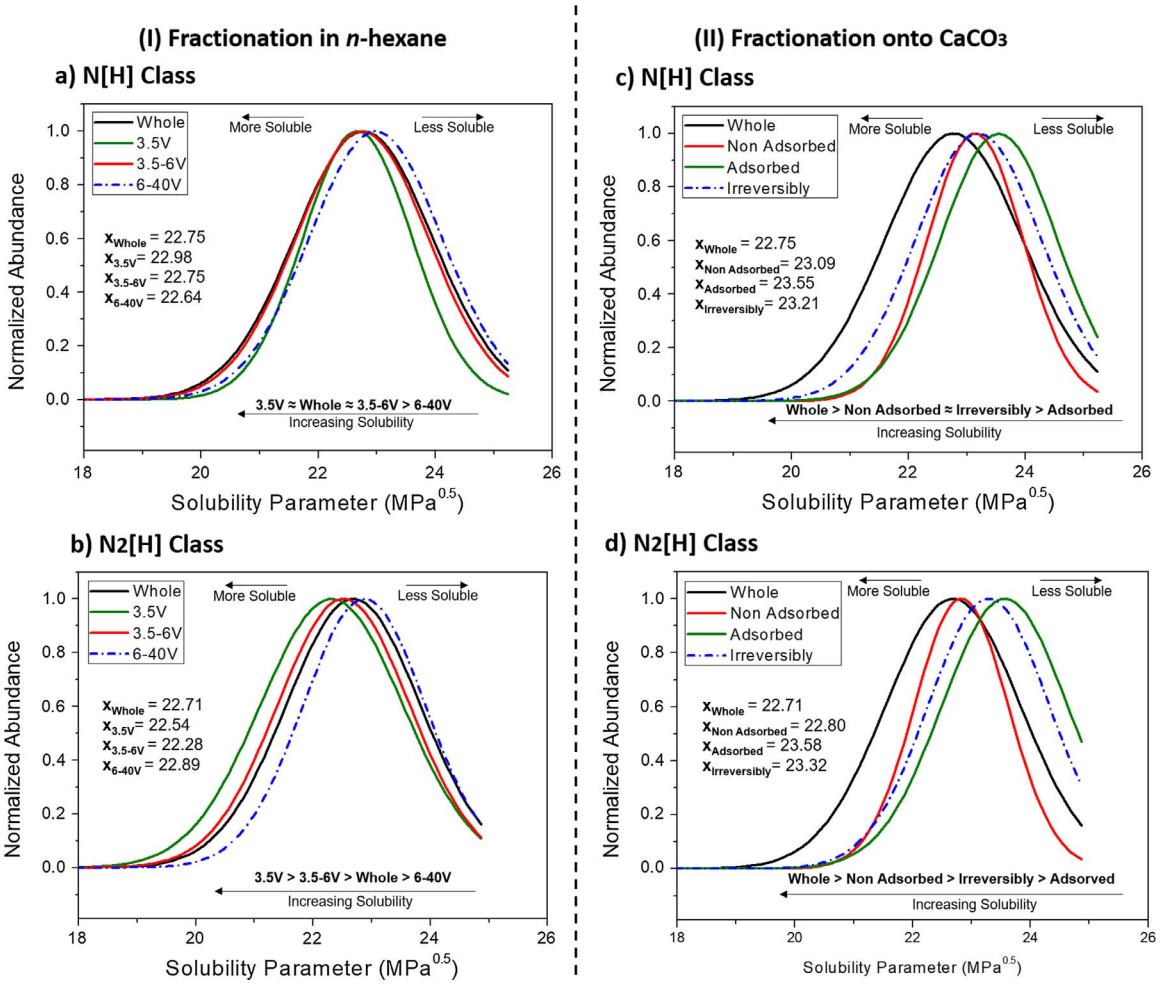

Fig. 8. Solubility parameters distribution for N[H] and N_2[H] classes for whole asphaltene and subfractions obtained by the fractionation in *n*-hexane (I) and onto $CaCO_3$ (II).

distribution for the N[H] class (Fig. 8a). Similar results were found for N_2[H] (Fig. 7b and Fig. 8b) and NO[H] classes (Fig. 5Sa).

The solubility parameters of the N[H] and N_2[H] classes of the subfractions obtained from fractionation onto $CaCO_3$ can be visualized in Fig. 7c–d, respectively, where the solubility increase in the following order: adsorbed < irreversibly adsorbed ~ non-adsorbed < whole asphaltene. A lower overlapping is now observed between the subfractions, where a shift to larger solubility parameters values can be noticed for irreversibly adsorbed and adsorbed subfractions, being an indication that these subfractions are less soluble in hydrocarbons. Analyzing the two-dimensional graphic of the solubility parameter distribution (Fig. 8c–d) this shift can be better visualized between the subfractions obtained using $CaCO_3$ as adsorbent Similar behavior was also observed for the NO[H] class (Fig. 5Sb).

4. Conclusion

Two methods of asphaltenes fractionation (in *n*-hexane and onto $CaCO_3$) were developed and compared, where their subfractions produced were characterized using elemental analysis, H^1 NMR, and ESI (+)FT-ICR MS data. The elemental analysis revealed that the C/H ratio for whole asphaltene and its sub-fractions varied between a narrow range (0.83–0.88) which means they present similar aromaticity or unsaturation. Furthermore, the elemental analysis corroborates with the ^{1}H NMR analysis suggesting that subfractions 6–40V and adsorbed onto $CaCO_3$ presented a more aromatic profile. However, a more detailed molecular information is obtained from ESI(+)-FT-ICR MS data, showing that a higher amount of polar compounds species with lower carbon number was mainly found for the irreversibly adsorbed subfraction obtained onto $CaCO_3$, thus suggesting, that it has the most polar species among the two fractionation methods studied. Besides, the DBE and CN distribution are important to associate the chemical information with solubility parameters, in which, when the DBE distribution became narrow, the subfractions became less soluble in hydrocarbons. Herein, this behavior was typically observed for irreversibly adsorbed (for fractionation onto $CaCO_3$) and subfraction 3.5V (fractionation in *n*-hexane) samples.

Solubility parameters (δ) was also calculated from ESI(+)FT-ICR MS data, where the subfractions presented an average solubility parameters values between 16 and 25 MPa$^{0.5}$. An overlapping of the N_x classes between the subfractions produced in *n*-hexane is observed, indicating that they have a lower tendency to precipitate in hydrocarbons about other produced onto $CaCO_3$. On the other hand, the subfractions, obtained from fractionation onto $CaCO_3$, present a lower overlapping for N_x class, among themselves, where a shift to larger solubility parameters can be noticed for irreversibly adsorbed and adsorbed subfractions. This indicates that they are less soluble in hydrocarbons due to their highest polar and aromatic character. The last was better visualized from van Krevelen diagrams. Our results show that the fractionation onto $CaCO_3$ procedure was able to produce more distinct subfractions, with different solubility parameters, aromaticity, and polarity. Future work will include the characterization of these subfractions by ESI(-), what will be Part 2 of this work.

Acknowledgments

Portions of this work were carried out as a part of the Joint Industrial Programme (JIP) Asphaltenes consortium "Improved Mechanisms of Asphaltene Deposition and Precipitation to Minimize Irregularities in Production and Transport – A Cost Effective and Friendly Approach sponsored by the Norwegian Research Council (234112/E30) and the following industrial sponsors: AkzoNobel, BP, Canada Natural Resources, Nalco Champion, Petrobras, Statoil and Total. Thanks are also due to FAPES (73309516/2016), Petrobras, CNPq, and CAPES (23038.007083/2014-40) for their financial support.

Appendix A. Supplementary data

Supplementary data associated with this article can be found, in the online version, at http://dx.doi.org/10.1016/j.fuel.2017.09.028.

References

[1] Silva SL, Silva AM, Ribeiro JC, Martins FG, Da Silva FA, Silva CM. Chromatographic and spectroscopic analysis of heavy crude oil mixtures with emphasis in nuclear magnetic resonance spectroscopy: a review. Anal Chim Acta 2011;707(1):18–37.
[2] Molnárné Guricza L, Schrader W. Electrospray ionization for determination of non-polar polyaromatic hydrocarbons and polyaromatic heterocycles in heavy crude oil asphaltenes. J Mass Spectrom 2015;50(3):549–57.
[3] Ferreira SR, Barreira FR, Spinelli LS, Leal KZ, Seidl P, Lucas E. Comparison between asphaltenes (sub) fractions extracted from two different asphaltic residues: chemical characterization and phase behavior. Quim Nova 2016;39(1):26–31.
[4] Pereira TM, Vanini G, Tose LV, Cardoso FM, Fleming FP, Rosa PT, et al. FT-ICR MS analysis of asphaltenes: Asphaltenes go in, fullerenes come out. Fuel 2014;131:49–58.
[5] He L, Lin F, Li X, Sui H, Xu Z. Interfacial sciences in unconventional petroleum production: from fundamentals to applications. Chem Soc Rev 2015;44(15):5446–94.
[6] Rogel E, Moir M, Witt M. Atmospheric pressure photoionization and laser desorption ionization coupled to fourier transform ion cyclotron resonance mass spectrometry to characterize asphaltene solubility fractions: studying the link between molecular composition and physical behavior. Energy Fuels 2015;29(7):4201–9.
[7] Qiao P, Harbottle D, Tchoukov P, Masliyah J, Sjoblom J, Liu Q, et al. Fractionation of asphaltenes in understanding their role in petroleum emulsion stability and fouling. Energy Fuels 2016http://pubs.acs.org/doi/abs/10.1021/acs.energyfuels.6b02401.
[8] Petrova LM, Abbakumova NA, Zaidullin IM, Borisov DN. Polar-solvent fractionation of asphaltenes from heavy oil and their characterization. Pet Chem 2013;53(2):81–6.
[9] Rogel E, Roye M, Vien J, Miao T. Characterization of asphaltene fractions: distribution, chemical characteristics, and solubility behavior. Energy Fuels 2015;29(4):2143–52.
[10] Kaminski TJ, Fogler HS, Wolf N, Wattana P, Mairal A. Classification of asphaltenes via fractionation and the effect of heteroatom content on dissolution kinetics. Energy Fuels 2000;14(1):25–30.
[11] Östlund JA, Wattana P, Nydén M, Fogler HS. Characterization of fractionated asphaltenes by UV–vis and NMR self-diffusion spectroscopy. J Colloid Interf Sci 2004;271(2):372–80.
[12] Subramanian S, Simon S, Gao B, Sjöblom J. Asphaltene fractionation based on adsorption onto calcium carbonate: part 1. Characterization of sub-fractions and QCM-D measurements. Colloids Surf A 2016;495:136–48.
[13] Tojima M, Suhara S, Imamura M, Furuta A. Effect of heavy asphaltene on stability of residual oil. Catal Today 1998;43(3):347–51.
[14] Okhotnikova ES, Ganeeva YM, Yusupova TN, Morozov VI, Frolov IN, Romanov GV. High-molecular-mass asphaltene fraction and its effect on the structure and stability of oxidized bitumens. Pet Chem 2011;51(3):187–91.
[15] Trejo F, Centeno G, Ancheyta J. Precipitation, fractionation and characterization of asphaltenes from heavy and light crude oils. Fuel 2004;83(16):2169–75.
[16] Trejo F, Ancheyta J. Characterization of asphaltene fractions from hydrotreated Maya crude oil. Ind Eng Chem Res 2007;46(23):7571–9.
[17] Fossen M, SjØblom J, Kallevik H, Jakobsson J. A new procedure for direct precipitation and fractionation of asphaltenes from crude oil. J Disper Sci Technol 2007;28(1):193–7.
[18] Pereira TM, Vanini G, Oliveira EC, Cardoso FM, Fleming FP, Neto AC, et al. An evaluation of the aromaticity of asphaltenes using atmospheric pressure photoionization Fourier transform ion cyclotron resonance mass spectrometry - APPI (±) FT-ICR MS. Fuel 2014;118:348–57.
[19] McKenna AM, Marshall AG, Rodgers RP. Heavy petroleum composition. 4. Asphaltene compositional space. Energy Fuels 2013;27:1257–67.
[20] Podgorski DC, Corilo YE, Nyadong L, Lobodin VV, Bythell BJ, Robbins WK, McKenna AM, Marshall AG, Rodgers RP. Heavy petroleum composition. 5. Compositional and structural continuum of petroleum revealed. Energy Fuels 2013;27:1268–76.
[21] Hsu CS, Hendrickson CL, Rodgers RP, McKenna AM, Marshall AG. Petroleomics: advanced molecular probe for petroleum heavy ends. J Mass Spectrom 2011;46(4):337–43.
[22] Savory JJ, Kaiser NK, McKenna AM, Xian F, Blakney GT, Rodgers RP, et al. Parts-per-billion Fourier transform ion cyclotron resonance mass measurement accuracy with a 'walking' calibration equation. Anal Chem 2011;83(5). 1732-1716.
[23] Cunico RL, Sheu EY, Mullins OC. Molecular weight measurement of UG8 asphaltene using APCI mass spectroscopy. Pet Sci Technol 2004;22(7–8):787–98.
[24] Purcell JM, Merdrignac I, Rodgers RP, Marshall AG, Gauthier T, Guibard I. Stepwise structural characterization of asphaltenes during deep hydroconversion processes determined by atmospheric pressure photoionization (APPI) Fourier transform ion cyclotron resonance (FT-ICR) mass spectrometry. Energy Fuels 2010;24:2257–65.
[25] Benassi M, Berisha A, Romão W, Babayev E, Rompp A, Spengler B. Petroleum crude oil analysis using low-temperature plasma mass spectrometry. Rapid Commun Mass Spectrom 2013;27:825–34.
[26] Colati KAP, Dalmaschio GP, de Castro EVR, Gomes AO, Vaz BG, Romão W. Monitoring the liquid/liquid extraction of naphthenic acids in Brazilian crude oil using electrospray ionization FT-ICR mass spectrometry (ESI FT-ICR MS). Fuel 2013;108:647–55.
[27] Freitas S, Malacarne MM, Romão W, Dalmaschio GP, Castro EVR, Celante VG, et al. Analysis of the heavy oil distillation cuts corrosion by electrospray ionization FT-ICR mass spectrometry, electrochemical impedance spectroscopy, and scanning electron microscopy. Fuel 2013;104:656–63.
[28] Dalmaschio GP, Malacarne MM, de Almeida VMDL, Pereira TMC, Gomes AO, de Castro EVR, et al. Characterization of polar compounds in a true boiling point distillation system using electrospray Ionization FT-ICR mass spectrometry. Fuel 2014;115:190–202.
[29] Haddad R, Regiani T, Klitzke CF, Sanvido GB, Corilo YE, Augusti DV, et al. Gasoline, kerosene, and diesel fingerprinting via polar markers. Energy Fuels 2012;26:3542–7.
[30] Klein GC, Kim S, Rodgers RP, Marshall AG. Mass spectral analysis of asphaltenes. II. Detailed compositional comparison of asphaltenes deposit to its crude oil counterpart for two geographically different crude oils by electrospray ionization fourier transform ion cyclotron resonance mass spectrometry. Energy Fuels 2006;20(5):1965–72.
[31] Kendrick E. A mass scale based on CH2 = 14.0000 for high resolution mass spectrometry of organic compounds. Anal Chem 1963;35(13):2146–54.
[32] da Silva Oliveira EC, Neto ÁC, Júnior VL, de Castro EVR, de Menezes SMC. Study of Brazilian asphaltene aggregation by nuclear magnetic resonance spectroscopy. Fuel 2014;117:146–51.
[33] Subramanian S, Sørland GH, Simon S, Xu Z, Sjöblom J. Asphaltene fractionation based on adsorption onto calcium carbonate: part 2. Self-association and aggregation properties. Colloids Surf A Physicochem Eng Asp 2017;514:79–90.
[34] Nascimento PT, Santos AF, Yamamoto CI, Tose LV, Barros EV, Gonçalves GR, et al. Fractionation of asphaltene by adsorption onto silica and chemical characterization by atmospheric pressure photoionization fourier transform ion cyclotron resonance mass spectrometry, Fourier transform infrared spectroscopy coupled to attenuated total reflectance, and proton nuclear magnetic resonance. Energy Fuels 2016;30(7):5439–48.
[35] Dias HP, Pereira TMC, Vanini G, Dixini PVM, Celante VG, Castro EVR, et al. Monitoring the degradation and the corrosion of naphthenic acids by electrospray ionization Fourier transform ion cyclotron resonance mass spectrometry and atomic force microscopy. Fuel 2014;85–95.
[36] Terra LA, Filgueiras PR, Tose LV, Romao W, de Souza DD, de Castro EVR, et al. Petroleomics by electrospray ionization FT-ICR mass spectrometry coupled to partial least squares with variable selection methods: prediction of the total acid number of crude oils. The Analyst 2014;139:4908–16.
[37] Panuganti SR, Vargas FM, Chapman WG. Property scaling relations for nonpolar hydrocarbons. Ind Eng Chem Res 2013;52:8009.
[38] Dudášová D, Simon S, Hemmingsen PV, Sjöblom J. Study of asphaltenes adsorption onto different minerals and clays: part 1. Experimental adsorption with UV depletion detection. Colloids Surf A 2008;317(1):1–9.
[39] Spiecker PM, Gawrys KL, Kilpatrick PK. Aggregation and solubility behavior of asphaltenes and their subfractions. J Colloid Interf Sci 2003;267(1):178–93.
[40] Gaspar A, Zellermann E, Lababidi S, Reece J, Schrader W. Impact of different ionization methods on the molecular assignments of asphaltenes by FT-ICR mass spectrometry. Anal Chem 2012;84(12):5257–67.
[41] Panda SK, Brockmann KJ, Benter T, Schrader W. Atmospheric pressure laser ionization (APLI) coupled with Fourier transform ion cyclotron resonance mass spectrometry applied to petroleum samples analysis: comparison with electrospray ionization and atmospheric pressure photoionization methods. Rapid Commun Mass Spectrom 2011;25(16):2317–26.
[42] Panda SK, Andersson JT, Schrader W. Characterization of supercomplex crude oil mixtures: what is really in there? Ang Chem Int Ed 2009;48(10):1788–91.
[43] Ikonomou MG, Blades AT, Kebarle P. Investigations of the electrospray interface for liquid chromatography/mass spectrometry. Anal Chem 1990;62:957–67.
[44] Pinto FE, Silva CFPM, Tose LVT, Figueiredo MAG, Souza WC, Vaz BG, et al. Evaluation of adsorbent materials for the removal of nitrogen compounds in vacuum gas oil by positive and negative electrospray ionization Fourier transform ion cyclotron resonance mass spectrometry. Energy Fuels 2017;31:3454–64.
[45] Rogel E, Witt M. Atmospheric pressure photoionization coupled to Fourier transform ion cyclotron resonance mass spectrometry to characterize asphaltene deposit solubility fractions: comparison to bulk properties. Energy Fuels 2016;30(2):915–23.
[46] Marshall AG, Rodgers RP. Petroleomics: chemistry of the underworld. Proc Natl Acad Sci 2008;105(47):18090–5.
[47] Klein GC, Kim S, Rodgers RP, Marshall AG, Yen A, Asomaning S. Mass spectral

analysis of asphaltenes. I. Compositional differences between pressure-drop and solvent-drop asphaltenes determined by electrospray ionization Fourier transform ion cyclotron resonance mass spectrometry. Energy Fuels 2006;20(5):1965–72.
[48] Van Krevelen DW. Graphical-statistical method for the study of structure and reaction processes of coal. Fuel 1950;29(12):269–84.
[49] Kim S, Kramer RW, Hatcher PG. Graphical method for analysis of ultrahigh-resolution broadband mass spectra of natural organic matter, the van Krevelen diagram. Anal Chem 2003;75(20):5336–44.
[50] Kim S, Rodgers RP, Blakney GT, Hendrickson CL, Marshall AG. Automated electrospray ionization FT-ICR mass spectrometry for petroleum analysis. J Am Soc Mass Spectrom 2009;20(2):263–8.
[51] Parra-Barraza H, Hernández-Montiel D, Lizardi J, Hernández J, Urbina RH, Valdez MA. The zeta potential and surface properties of asphaltenes obtained with different crude oil/n-heptane proportions. Fuel 2003;82(8):869–74.